Particle Concentration and Characteristics near a Major Freeway with Heavy-Duty Diesel Traffic

ARTICLE *in* ENVIRONMENTAL SCIENCE AND TECHNOLOGY · MAY 2007

Impact Factor: 5.33 · DOI: 10.1021/es062590s · Source: PubMed

4 AUTHORS, INCLUDING:

Zhi Ning
City University of Hong Kong
59 PUBLICATIONS **1,221** CITATIONS
SEE PROFILE

Michael D Geller
United States Environmental Protection Age…
31 PUBLICATIONS **1,226** CITATIONS
SEE PROFILE

Constantinos Sioutas
University of Southern California
316 PUBLICATIONS **14,844** CITATIONS
SEE PROFILE

Particle Concentration and Characteristics near a Major Freeway with Heavy-Duty Diesel Traffic

LEONIDAS NTZIACHRISTOS, ZHI NING, MICHAEL D. GELLER, AND CONSTANTINOS SIOUTAS*

Department of Civil and Environmental Engineering, University of Southern California, Los Angeles, California 90089

This study presents the number, surface and volume concentrations, and size distribution of particles next to the I-710 freeway during February through April 2006. I-710 has the highest ratio (up to 25%) of heavy-duty diesel vehicles in the Los Angeles highway network. Particle concentration measurements were accompanied by measurements of black carbon, elemental and organic carbon, and gaseous species (CO, CO_2). Using the incremental increase of CO_2 over the background to calculate the dilution ratio, this study makes it possible to compare particle concentrations measured next to the freeway to concentrations measured in roadway tunnels and in vehicle exhaust. In addition to the effect of the dilution ratio on the measured particle concentrations, multivariate linear regressions showed that light and heavy organic carbon concentrations are positively correlated with the particle volume in the nucleation and accumulation modes, respectively. Solar radiation was also positively correlated with the particle surface concentration and the particle volume in the accumulation (40−638 nm) mode, presumably as a result of secondary particle formation. The methods developed in this study may be used to decouple the effect of sampling position, meteorology, and fleet operation on particle concentrations in the proximity of freeways, roadway tunnels, and in street canyons.

Introduction

Various epidemiological studies have concluded that a positive correlation exists between airborne particulate matter (PM) and adverse effects on human health (*1*, *2*). Recent toxicological studies corroborate these findings both in vitro and in vivo (*3*, *4*). Although this compelling evidence exists, the causal mechanisms behind these toxic responses remain uncertain. Consequently, which metric of PM—mass, surface area, or number of particles—may be responsible for toxicity remains unknown. Recent studies suggest that ultrafine particles (d_p < 100 nm) may elicit a higher adverse response per unit mass than fine (d_p < 2.5 μm) and coarse (2.5 μm < d_p < 10 μm) particles (*5*, *6*).

Dynamometer experiments have shown motor vehicles to emit high concentrations of particles by number, and heavy-duty diesel vehicles (HDVs) without particle traps, in particular, emit high PM mass concentrations (*7*, *8*). Recently, sampling conducted in freeway microenvironments has also confirmed high concentrations of PM due to motor vehicles (*9*, *10*). Zhu et al. (*9*) found that particle number concentration was highly influenced by distance from the freeway, with a large spike in particle number next to the roadway that decays to background levels within 100−150 m. $PM_{2.5}$ (particulate matter less than 2.5 μm in aerodynamic diameter) mass concentration was nearly unaffected over the same distances. Westerdahl et al. (*10*) reported concentrations of PM and various co-pollutants while driving on various roads and highways in Los Angeles. Concentrations on some of the freeways sampled in that study peaked as high as one million particles per cm^3. Thus, it has been suggested that exposure to motor vehicle exhaust emissions during commute constitutes a large fraction of daily personal PM exposure, especially to ultrafine PM.

The vast freeway network in Los Angeles accommodates over six million registered vehicles. Therefore, it is reasonable that most $PM_{2.5}$ originates from vehicles, which has been proven in other urban areas (*11*, *12*). PM is both directly emitted, via combustion and mechanical wear, and formed via secondary reactions of direct emissions, whereby organic and inorganic vapors undergo gas-to-particle conversion in the atmosphere (*13*, *14*). Roadways with high HDV traffic have been shown to have elevated particle number and mass concentrations, and especially high levels of black carbon (*10*).

In this study, detailed information is provided on the physical and chemical characteristics of particles originating from a major freeway during the winter season, with a significant HDV fraction. This was accomplished by measuring semi-continuous and time-integrated particle number, surface area, mass,and chemistry adjacent to I-710 from February to April 2006. The results are compared to those of previous studies, after correcting for the dilution ratio in different sampling locations, and a regression analysis is conducted to reveal the effect of meteorology and traffic conditions on the observed particle concentrations.

Materials and Methods

The I-710 freeway is a 26 m wide eight-lane highway connecting the ports complex of Long Beach and San Pedro to the shipping yards in East Los Angeles. For this reason, as much as 25% diesel traffic has been reported on this freeway (http://traffic-counts.dot.ca.gov). Total traffic counts are also very high, with between 150,000 and 200,000 vehicles per day passing the sampling location. The sampling site was located in a paved property run by the Imperial Flood Control Yard in South Gate, CA. This location, shown in Figure 1, is directly adjacent to the roadway with no other immediate sources either upwind or downwind. Just downwind of the site are a bike path and the Los Angeles River, a concrete-lined drainage channel.

To ensure that sample probes were within the plume of the freeway, wind speed and direction were monitored with a portable weather station (Monitor II, Weather Systems Company, San Jose, CA). This instrument also recorded local temperature and relative humidity. Data were logged over 5 min intervals during the entire study. The monitor was located 2 m above the ground, and direction was calibrated daily by aligning the weather vane with a compass.

Traffic data were collected by two methods that were used to create a comprehensive traffic profile. Total traffic volume (including all vehicle types) and average vehicle speed were obtained from the California Department of Transportation

* Corresponding author e-mail: sioutas@usc.edu; fax: (213) 744 1426.

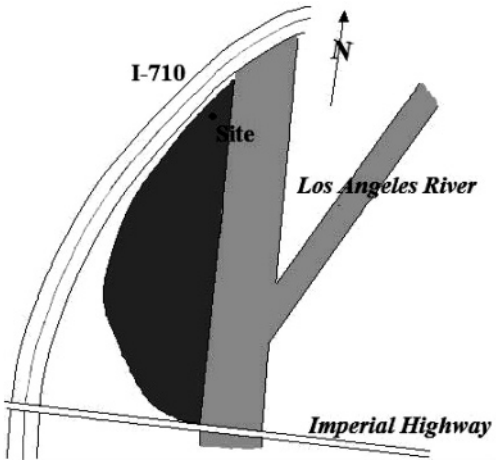

FIGURE 1. Sampling site in the proximity of the I-710 freeway.

(Caltrans, www.dot.ca.gov), which has vehicle loop sensors positioned along the freeway at a location within a mile of the sampling site. Manual and videotaped counts were also taken for 1 min out of every 5 min during randomly selected sampling intervals. Estimates of traffic counts broken down by vehicle type were done by analyzing the videotapes and counting the number of axles per vehicle.

Both gaseous and particulate pollutant concentrations were measured with various continuous and time-integrated instruments, approximately 10 m from the shoulder of the freeway. The prevailing southwesterly winds transported the fresh freeway emissions to the sampling location. Instruments were located in a retrofitted box truck that was driven to the site each day. Copper and antistatic tubes were extended approximately 1 m above the truck's roof to ensure representative sampling. Tubing diameter was chosen such that the approximate residence time was less than 1 s in the sampling lines.

Table 1 lists the instruments used in this study and the species sampled. The continuously measured gas species included carbon monoxide (CO) and carbon dioxide (CO_2). CO/CO_2 measurements were recorded with handheld air quality monitors (Q-Trak Plus). The Q-Traks were calibrated both before and during the study period by performing zero and span checks, with gas standards provided by the manufacturer. Additionally, the Q-Traks were frequently connected to zero and span gases to confirm that no drift was occurring over the course of the study. Particle size distributions in the range 16 to 638 nm (mobility diameter) were recorded every 120 s by a Scanning Mobility Particle Sizer (SMPS), using a sample flowrate of 0.3 L/ min^{-1} and a sheath flowrate of 3.0 L min^{-1}. A Condensation Particle Counter (CPC) recorded continuous total particle counts. Particle number and mass (by assuming an average density of 1.0 g cm^{-3}) concentrations in the range of 0.7−2.5 μm (aerodynamic diameter) were measured in 5 min intervals by means of the Aerodynamic Particle Sizer (APS). Particle number concentrations by both SMPS and APS were determined by integrating over the particle number size distribution. Continuous particle surface concentration was measured with the recently developed Nanoparticle Surface Area Monitor (NSAM). This measures the total particle surface area available for diffusion of ions. A dual beam aethalometer measured black carbon (BC) concentrations every 5 min. In addition, an organic carbon (OC)/elemental carbon (EC) field instrument (OC/EC) measured hourly $PM_{2.5}$ elemental and organic carbon concentrations. This instrument allows for the separation of particulate OC into four response peaks representing different volatility fractions of OC (*15*). For the purposes of this study, peaks 2−4 were summed and considered as the least volatile or heavy OC fraction (HOC), while peak 1 represented the lighter, most volatile OC fraction (LOC).

Results and Discussion

Particle and Co-Pollutant Concentrations Next to the Freeway. Meteorological and traffic parameters were measured during the course of sampling. The average wind direction was 215 ± 39 degrees, which placed the sampling site directly downwind of freeway traffic emissions, and the mean wind speed was 1.8 ± 0.9 ms^{-1} (all ranges given as mean ± standard deviation). The temperature and relative humidity were 19.6 ± 5.0 °C and 46.2 ± 16.3%, respectively, with a diurnal profile shown later in the paper. Caltrans reported total volumes of north- and south-bound lanes in the range of 5180 ± 640 h^{-1} and 5640 ± 800 h^{-1}, respectively. The average traffic speeds of north and south bound lanes were 78 ± 28 km h^{-1} and 85 ± 12 km h^{-1}, respectively. Video recordings revealed that 11−21% of vehicles on the freeway were HDVs. However, when expressed as an absolute hourly density on the freeway, the HDV number did not significantly differ during the sampling hours (1700−2160 h^{-1}). This range is slightly lower than previously reported in studies conducted in 2001 (*16*) on the same freeway, possibly due to the opening of a railway line (Alameda Corridor) in 2002, which is used for the transport of goods from the Los Angeles port.

Table 2 presents the mean particle and copollutant levels measured near the freeway over the 7-week sampling period (120−140 h of data, depending on the magnitude considered). The average CPC particle number concentration was 86 000 cm^{-3} during the course of the whole campaign whereas the average SMPS concentration was 19 000 cm^{-3}. The difference between the two instruments can be attributed to the different size ranges (CPC > 6 nm, SMPS 16−638 nm) and particle losses in the SMPS, and it is a strong indication that the particle concentration near the freeway is dominated by particles less than 16 nm in diameter. The high particle number concentration below 16 nm is consistent with the results of Zhu et al. (*9*), conducted in the winter of 2002 next to the same freeway. The particle surface concentration measured with the NSAM was 153 ± 55 μm^2 cm^{-3}. With regard

TABLE 1. Instrumentation Used and Species Measured during the Study

instrument	model/manufacturer	species sampled
Q-Trak Plus	8554, TSI Inc.	CO, CO_2, temperature, relative humidity
SMPS	3936L, consisting of DMA 3081L and CPC 3022A, TSI Inc.	particle number/size distribution (16−638 nm mobility)
CPC	3022A, TSI Inc.	number concentration (>6 nm mobility)
APS	3020A, TSI Inc.	particle number/size distribution (0.7−2.5 μm aerodynamic)
NSAM	3550, TSI Inc.	particle active surface concentration (<∼1 μm aerodynamic)
OC/EC	3F/Sunset Labs Inc.	organic and elemental carbon
Aethalometer	AE-20/Anderson Instruments Inc.	black carbon

TABLE 2. Summary of Particle and Copollutant Levels Next to the Freeway for the Three Cases: Campaign, a Rainy Day, and a Day When the Freeway Was Closed

	campaign average			rainy day			freeway closed		
	average	range	SD[a]	average	range	SD[a]	average	range	SD[a]
N_{CPC} (cm^{-3})	8.6×10^4	$1.1 \times 10^4 - 3.2 \times 10^5$	5.4×10^4	3.4×10^4	$1.3 \times 10^4 - 8.3 \times 10^4$	2.2×10^4	3.1×10^4	$2.5 \times 10^4 - 3.8 \times 10^4$	6.8×10^3
N_{SMPS} (cm^{-3})	1.9×10^4	$3.7 \times 10^3 - 5.4 \times 10^4$	9.4×10^3	5.5×10^3	$2.3 \times 10^3 - 1.0 \times 10^4$	3.0×10^3	6.5×10^3	$5.1 \times 10^3 - 8.0 \times 10^3$	1.4×10^3
$PM_{0.7-2.5}$ ($\mu g/m^3$)	6.4	1.7−30	3.6	8.2	6.7−8.8	0.85	2.1	1.7−2.3	0.27
surface ($\mu m/cm^3$)	153	36−303	55	41	20−64	19	57	45−71	12
V_{NM} ($\mu m^3/cm^3$)	0.094	0.011−0.22	0.047	0.031	0.011−0.061	0.02	0.049	0.035−0.058	0.13
V_{AM} ($\mu m^3/cm^3$)	16.3	3.66−36.5	6.96	7.1	4.73−9.79	1.86	4.3	3.7−5.6	1.1
Geomean d_p (nm)	50	28−96	11	53	40−60	7	46	42−52	4
EC ($\mu g/m^3$)	3.2	0.3−11.2	2.2	0.7	0.3−1.15	0.3	0.40	0.3−0.5	0.2
BC ($\mu g/m^3$)	4.4	0.5−10.1	2.1	2.6	0.8−9.8	2.8	0.8	0.8	<0.1
LOC ($\mu g/m^3$)	2.4	0.9−5.3	0.8	1.3	1.1−1.7	0.2	3.0	2.8−3.2	0.3
HOC ($\mu g/m^3$)	2.0	0.1−11.2	1.4	1.2	0.9−1.8	0.3	1.6	1.5−1.8	0.2
CO (ppmv)	0.23	0.10−3.6	0.35	0.01	<0.09	0.02	0.29	<1.2	0.53
CO_2 (ppmv)	426	359−567	30	402	384−430	14	405	401−410	3.6

[a] Standard deviation.

to carbon species, BC concentration measured 4.4 ± 2.1 μg m^{-3}, which is at similar levels with EC (3.2 ± 2.2 μg m^{-3}) and total OC (4.4 ± 1.6 μg m^{-3}). The fraction of EC and BC to $PM_{0.7-2.5}$ was 50% and 68%, respectively. In a previous study at the Caldecott tunnel (*17*) with 3−6% diesel vehicles, EC accounted for 30−38% of $PM_{2.5}$. It was also reported that, on average, BC accounted for 50% of PM_3 at the entrance and 30% at the exit in Gubrist tunnel with 16% diesel vehicles (*18*). EC is considered a marker for diesel exhaust aerosol emissions in tunnels (*19*), and the results presented in this study are consistent with earlier studies with similar diesel fractions.

Table 2 also shows the volumes of nucleation (16−40 nm) and accumulation (40−638 nm) mode particles, calculated from the SMPS distributions. By combining the volume of accumulation mode particles with the effective particle density, we obtain an estimation of the particle mass in this size range. Next to the 710 freeway, the effective density of particles in the 322−414 nm mobility range, where most of the accumulation mode volume resides, varies between 0.49 and 0.31 g cm^{-3} (*20*). Using this density range, the particle mass in the accumulation mode is calculated to have been between 5.0 and 8.0 μg m^{-3}, which is within the range of the sum of EC and TOC concentrations shown in Table 2. This suggests that these two species accounted for the majority of particle mass in that location and for that size range.

Particle and copollutant concentrations during two special events are also included in Table 2. During freeway closure, which occurred for a single day (March 8) due to police activity, the particle number, mass, and surface area concentrations significantly dropped due to the absence of the most dominant particle emission sources, given that there are no other significant ultrafine particle sources in that area (*9*). Average EC and BC also declined to levels much lower than the whole campaign average, thus demonstrating that vehicle activity on the freeway is their main source. However, OC species did not decline as much, indicating that there are some significant sources of background organic carbon, including, for example, secondary organic aerosols (SOA) as well as existing background concentration due to "aged" OC produced in previous days that had yet to be transported out of the Los Angeles Basin. A second special occasion occurred for a rainy day (March 20), when sampling took place during light rain conditions. Rain led to particle scavenging from the atmosphere, resulting in a decrease in particle number and surface area concentrations.

Diurnal Profiles. Figure 2 shows the averaged diurnal trends of the various parameters categorized as (a) meteorological and (b) traffic conditions, and (c) particle chemical and (d) physical properties. The *y*-axis is the normalized value of the different parameters with $y = 100$ equal to the values listed in brackets for each parameter. The *x*-axis in the figures shows the sampling hour, which ranges from 11:00 to 19:00. As the day progressed, relative humidity increased while the temperature and solar radiation decreased. Wind speed was consistent throughout the day with a small peak in the early afternoon while total traffic volume on the freeway was consistent during the sampling period, with slight increases during morning and afternoon rush hours. The average speed in the north-bound lane dropped during congestion, between 15:00 and 17:00. In Figure 2b, the "CO_2 Production" profile corresponds to the total CO_2 production rate (tons/h) per km due to the vehicle activity. This has been calculated on the basis of activity data provided by Caltrans for driving speeds and traffic volume, the split in diesel HDV and gasoline cars, and appropriate CO_2 emission functions for each vehicle category (*21*). The total CO_2 production changed very little during the study, due to the relatively constant speeds and traffic volumes during the day. During congestion, the CO_2 production rate increased mildly due to the acceleration−deceleration driving pattern. However, the increase is not substantial due to the relative reduction of the total traffic volume.

Both EC and BC average concentrations display a bimodal pattern and agree with each other very well, indicating identical sources of EC and BC (Figure 2c). Two peaks were observed at 11:00 and later in the afternoon (15:00−16:00) corresponding to the diurnal pattern of the traffic rush hours. The diurnal patterns of OC species do not follow traffic as closely and this is a further indication that these may come from both direct traffic emissions as well as secondary formation mechanisms through photochemical reactions.

With regard to particle concentrations, SMPS total number concentration, surface concentration, and volume of nucleation and accumulation modes all peaked at 16:00 when traffic was congested. These associations strongly indicate the link between particle concentrations and traffic emission on the freeway. Harrison et al. (*22*) have also reported that roadside particle number and surface concentrations have the same general pattern of behavior as the vehicle emission source. On the other hand, the CPC number concentration showed a monotonically increasing trend from 50,000 cm^{-3} to 110,000 cm^{-3} as the day progressed. This can be explained by the nucleation process of small particles with decreasing temperature in the evening. Similar results have also been observed by Kuhn et al. (*23*). These results indicate that the

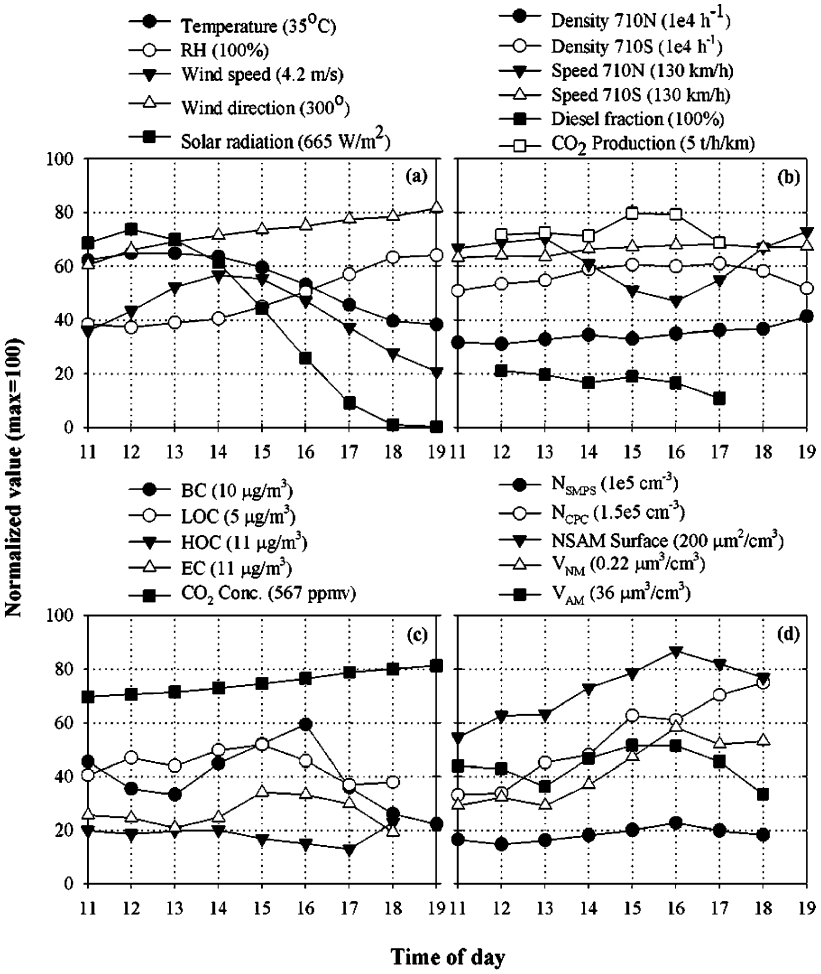

FIGURE 2. Diurnal profile of measured variables normalized over the maximum hourly value recorded (given in the legend within parentheses): (a) meteorological conditions, (b) traffic data, (c) particle chemical parameters and CO_2, and (d) particle physical parameters.

TABLE 3. Comparison of Concentrations in Different Studies Involving Heavy-Duty Diesel Vehicle Traffic (Italicized Values Have Been Corrected for the Different Dilution Ratios, Calculated on the Basis of the CO_2 Concentrations)

	2006 study		Westerdahl et al. (*10*)	Geller et al. (*24*)
location	I-710		I-710	Caldecott Tunnel (Bore 1)
sampling site	20 m from freeway median strip		mobile lab following traffic	tunnel exit
period	Feb–Apr 2006		Feb–Apr 2003	Aug 2004
sampling hours	12 pm–4 pm	5 pm–7 pm		12 pm–6 pm
passenger cars (h^{-1})	8359	10250	7580[a]	4041
light-duty trucks (h^{-1})	600	360		91
heavy-duty trucks (h^{-1})	1630	1225	1040[a]	64
temperature (°C)	21.4	14.4	21	23.3
RH (%)	42	60		59
wind speed (m/s)	2.2	1.2	2.0	

	measured	measured	measured	corrected for DR[b]	measured	corrected for DR[b]
CPC (cm^{-3})	75000	98500	190000	*36600 (5400)*	637500	*92600 (10100)*
CO (ppm)	0.27	0.11	1.9	*0.28 (0.05)*	8.78	*2.18 (0.21)*
BC ($\mu g/m^3$)	4.6	2.8	12	*3.4 (0.6)*	27.5[c]	*6.8 (1.4)*
relative dilution ratio	1:1			*1:10.2 (1.22)*		*1:7.3 (0.82)*

[a] Daily averages from CalTrans. [b] Values in parentheses correspond to calculation uncertainty (see Supporting Information). [c] Elemental carbon.

particle concentration and characteristics next to the freeway are influenced by a combination of the traffic activity and the meteorological conditions. The statistical analysis presented in a following section will help to further identify the underlying associations.

Comparison with Previous Studies. Particle characterization studies in the vicinity of freeways or tunnels with diesel HDV traffic have been conducted in the past. Westerdahl et al. (*10*) measured particle characteristics by driving a mobile lab on fixed routes in the Los Angeles road network, including a stretch of the I-710 freeway where they chased different vehicle plumes. In another study, Geller et al. (*24*) measured size distributions in the Caldecott tunnel (Bore 1), located in Orinda, CA. Table 3 compares measured particle

number and copollutant concentrations from these two studies to the current one. All studies were conducted under similar temperature and relative humidity conditions and the wind-speed was also very similar in the two non-tunnel studies. The diesel truck fraction was ~3.7% in the Caldecott tunnel, and the road had a positive gradient of +4.2%.

It is important to correct for the dilution ratio (DR) in the various sampling locations before comparing pollutant concentrations between these studies. This correction enables us to decouple the effects of fleet operation and ambient conditions on pollutant levels from the influence of the exact position of the monitoring station. The DR calculation is based on the ratio of the fleet-average exhaust CO_2 concentration over the incremental ambient CO_2 increase, and it is given as Supporting Information. Carbon dioxide has been used in several studies as a tracer to derive fuel-specific emissions from ambient pollutants concentrations (*25*) or to deduce emission factors in tunnel measurements (*26*). While the fundamentals of those approaches are similar to our study, we use the incremental increase in ambient CO_2 to deduce dilution conditions in different environments. The calculations show that the DR by the freeway (present study) is 10.2 ± 1.22 times higher than in-freeway, and 7.3 ± 0.83 times higher than in the tunnel. These ratios are consistent with the conceptual model of Zhang et al. (*27*), who estimated that the road-to-ambient process is associated with an additional DR of ~10.

Concentrations varied in the range 75 to 637.5 thousand particles per cm^3 in the different studies before correcting for the DR. After correction (italicized values in Table 3), concentrations reached rather similar levels, which can lead to interesting conclusions. The in-freeway concentrations of particle number and BC measured by Westerdahl et al. (*10*) are lower than the values of this study while CO is at the same levels. This may be attributed to the different mixing of the exhaust when sampling in the freeway as opposed to next to the freeway. When following traffic, there is a larger probability to follow a car than a truck, due to the larger density of passenger cars. The different mixing would have a limited effect on the DR calculated, since the CO_2 concentration in the exhaust of the two vehicle types is different (gasoline, 12.5%; diesel, 7.1%). However, it is not possible to calculate a more precise DR than the one corresponding to mean fleet operation (Table S2), unless the probabilities of following a car vs a truck plume are known. Nevertheless, the effect of different mixing on DR is negligible compared to the orders of magnitude difference expected for the concentration of BC and particle number in the exhaust of the two vehicle types. Therefore, the higher CO/BC ratio of the Westerdahl et al. (*10*) study, compared to the present results, is suggestive of the larger CO/BC ratio from gasoline vehicles. This is consistent with the much higher ratio of CO over light extinction by the exhaust plume of gasoline compared to diesel vehicles (*28*). For the same reason, the DR-corrected particle number concentration is lower than that measured next to the freeway, which is due to the lower on-road particle number emission factors of gasoline cars vs diesel trucks (*24*, *29*).

On the other hand, the particle number and BC concentration in the Caldecott tunnel are at the same or slightly higher levels than next to the freeway after DR correction, despite the much lower fraction of diesel vehicles in the tunnel. This is most probably due to the uphill driving in the tunnel, which has a significant effect on the engine load. Using typical values for road resistance and solving the equation of motion for LGVs and HDDVs (see Supporting Information), 4.2% positive road gradient corresponds to ~1.6 times increase in engine load for a light duty gasoline engine and a ~2.9 increase for a diesel truck engine. The high particle number concentrations in this case are consistent with the findings of Kittelson et al. (*29*) and Maricq et al. (*8*), who show a large increase in particle number from gasoline vehicles as the engine load increases. The effect of engine load on particle number concentration is not as significant in diesel engines (*7*) but does increase BC emissions (*30*), which leads to the relatively high ambient concentration of BC, despite the small fraction of diesel vehicles.

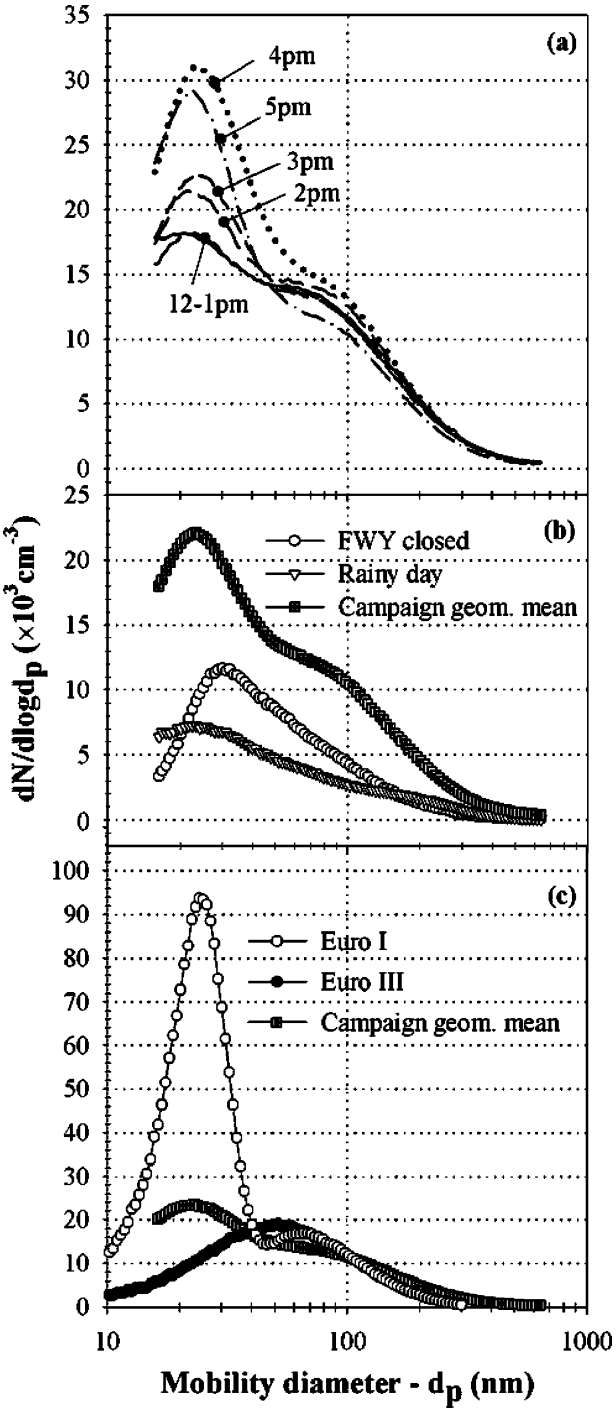

FIGURE 3. (a) Mean geometric hourly size distributions measured during the 7-week campaign, (b) effect of individual events on the particle size distributions, and (c) comparison of the grand average size distribution measured next to the freeway with typical exhaust size distributions of two heavy-duty vehicles measured in the laboratory, after correction for the dilution ratio.

Particle Size Distributions. Figure 3 shows particle size distributions obtained next to the freeway during different hours of the day (panel a), over different special events (panel

TABLE 4. Multiplication Coefficients for the Standardized Independent Variables Used to Formulate the Reconstructed Concentrations (Values in Parentheses Correspond to One Standard Deviation for the Corresponding Variable)

	reconstructed variables			
independent variables	CO_2 (24 ppmv)	surface (61.4 μm/cm^3)	V_{AM} (7.2 μm^3/cm^3)	V_{NM} (0.049 μm^3/cm^3)
wind speed (0.90 m/s)	−0.24			−0.18
wind direction (32°)	+0.53			
solar radiation (209 W/m^2)	−0.38	+0.21	+0.35	
BC (2.0 μg/m^3)		+0.23	+0.46	+0.33
LOC (0.79 μg/m^3)		+0.36		+0.22
HOC (0.96 μg/m^3)			+0.24	
CO_2 (24 ppmv)		+0.68	+0.49	+0.51

b), and, finally, in comparison to HDV particle exhaust distributions measured in the laboratory (panel c). The ambient particle distributions (campaign grand average and hourly averages) are the geometric mean of the corresponding size distributions recorded over the 7-week sampling period.

Figure 3a shows that the particle size distribution next to the diesel freeway was bimodal, with a nucleation mode in the size range below 40−50 nm and an accumulation mode peaking at 70−80 nm during all sampling hours. This bimodal distribution has been typically encountered in the proximity of freeways with diesel traffic (*9*) or when following a diesel vehicle on the road (*31*−*33*) but has not been present when sampling in the proximity of a gasoline freeway (*23*). During freeway closure (Figure 3b), there was no traffic-induced emission source and the particle concentration dropped significantly compared to the average. In addition, the size distribution became monomodal within the range 16−638 nm studied, with a peak concentration of 12,000 cm^{-3} at 30 nm. During the rainy day, the concentration of the whole size distribution dropped by 70%, similar to the observations of Mozurkewich et al. (*34*).

Figure 3c attempts to explain the bimodal size distribution by comparing the average size distribution recorded next to the 710 freeway to typical size distributions obtained by older technology (Euro I) and more recent technology (Euro III) HDVs (*35*). These distributions correspond to mode 5 of the European heavy-duty Stationary Cycle (ESC 5), which stands for moderate speed (∼60% of maximum speed) and 50% load, both typical of freeway driving. The exhaust concentrations have been corrected for the DR considered at the sampling location (1917 ± 219; Supporting Information) and the contribution of HDV exhaust flowrate to the mean fleet exhaust flowrate. The comparison shows excellent agreement in the size range of both particle modes, between freeway and laboratory sampling. In addition, the concentration of particles larger than 40−50 nm (accumulation mode) measured in the laboratory is very close to the levels measured next to the freeway. However, the accumulation mode distribution is wider next to the freeway than in the laboratory studies, which may be due to the averaging effect on the size distributions of several vehicles, and/or to the contribution of other particle sources (secondary particles and non-exhaust vehicle particles).

With regard to the nucleation mode particles, the size range determined in the laboratory from the Euro I engine (employing a primary DR of 12.5:1, a dilution temperature of 32 °C, and a residence time of 2.5 s) is similar to the size distribution measured next to the freeway. However, the actual number concentration depends on the vehicle technology and the sampling conditions. In addition, the nucleation mode formed next to the freeway also depends on species emitted by gasoline vehicles.

The comparison of the tunnel, on-road, dynamometer, and present studies demonstrates that the measurement of the incremental increase in ambient CO_2 due to traffic is a good indicator of the DR at the sampling location and can be used to infer concentrations at other locations with similar conditions. This can be used to decouple the effect of sampling position from the difference in the measured pollutant levels.

Statistical Processing of the Sampled Variables. A multivariate linear regression analysis was performed on a dataset of 86 hourly average values of traffic, ambient, and pollutant concentration data, in order to associate particle concentrations next to the freeway with traffic and ambient conditions as well as co-pollutant concentrations. The dataset size was limited to 86 h because it was necessary to have a complete set of values for all 22 variables recorded during sampling. The variables included all magnitudes shown in Figure 2, with the addition of the $PM_{0.7-2.5}$ mass and the time of sampling. "CO_2 Production" was excluded because it was not possible to have a precise estimate for each hour of the sampling period. The dependent variables considered in the regressions were the CO_2 concentration, the CPC particle number, the surface concentration, and the volumes of particles in the nucleation (16−40 nm) and accumulation (40−638 nm) modes. All other recorded variables were considered independent. For the CO_2 regression in particular, only traffic data and ambient conditions were considered as independent variables. All regressions were carried out with SPSS 12.0 and only final linear combinations at a confidence level of 99.5% were considered.

The results of the multivariate linear regression analysis are shown in Table 4. The values in the table correspond to the multiplication factors for the standardized independent variables (input). The linear combination of the multiplication factor and the standardized input variable leads to a reconstructed value of the dependent variable. The correlation of the dependent (measured) variables and the reconstructed variables is satisfactory with regression slopes on the order of 0.91−1.0 and R^2 above 0.6 (Figure S2 in Supporting Information). However, it was not possible to derive a reconstructed variable that would satisfactorily correlate with the CPC particle number. This is probably because the nucleation of new particles is a highly sensitive, nonlinear function of the input variables, and it is therefore not possible to linearly associate it with the independent variables considered.

Given the satisfactory correlations between the reconstructed and the dependent variables, the values in Table 4 may be used to establish the associations of the dependent with the independent variables. The multiplication coefficients in this table correspond to standardized variables. For example, a decrease in the wind speed by one standard deviation (which corresponds to a variation of 0.9 m/s) would increase the CO_2 concentration by 0.24 standard deviations (which corresponds to an increase of 0.24 × 24 ppm = ∼5.8 ppm). Based on these values, it is evident that CO_2 concentration increases as wind speed decreases, as wind direction changes toward the west (moving the sampling point closer

to the freeway), and in the afternoon and evening hours as the sun sets and the mixing height decreases. These relationships confirm that CO_2 is a very good indicator of the DR. Interestingly, CO_2 concentration does not depend on the traffic volume and conditions because there was little variation of the CO_2 emitted per hour on the highway, as shown in Figure 2b (standard deviation over mean was 13% for the whole measurement campaign). Presumably, this variation is not high enough to cause a measurable difference in the CO_2 concentration levels.

The CO_2 concentration was then used as an independent variable to reconstruct the concentration of the particle surface and volume concentrations. Table 4 shows that all three particle concentration expressions are positively affected by the CO_2 concentration, which is consistent with an increase in the concentration of these variables with decreasing DR. All concentrations are also positively associated with BC. Interestingly, LOC is positively associated with the nucleation mode volume, while HOC is associated with the accumulation mode. There is evidence (*30*, *36*) that the gasoline OC profile is shifted to heavier species than the diesel one. This would imply that the nucleation mode volume in the size range 16−40 nm is mainly associated with the diesel activity on the freeway. This is consistent both with the laboratory measurements (Figure 3c) and with the findings of Zhu et al. (*9*) who found that next to the diesel freeway (I-710) a distinct particle mode appears in the 20−30 nm range. This mode is clearly separated by a higher nucleation mode forming below 10 nm and was not evident when sampling next to a (mainly) gasoline freeway (I-405). It needs to be noted that a high particle concentration below 16 nm is also evident in our study when comparing the CPC and SMPS recordings. Unfortunately, due to the lack of linear correlation of the CPC recordings with any of the other measured variables, it was not possible to link the origin of this nanoparticle (6−16 nm) mode to either diesel or gasoline vehicles.

The regression analysis also shows that the NM volume concentration is negatively correlated to the wind-speed. This is in addition to the effect of wind on dilution, expressed by the CO_2 correlation, and can be an indication of NM evaporation as the wind-speed increases. Finally, the volume of accumulation mode is positively correlated with the solar radiation. This indicates that there may be other processes, unrelated to traffic, that contribute to a significant portion of the aerosol in that size range, such as secondary formation by photochemical activity.

Acknowledgments

This research was supported by the Southern California Particle Center (SCPC), funded by EPA under the STAR program through Grant RD-8324-1301-0 to the University of Southern California. The research described herein has not been subjected to the agency's required peer and policy review and therefore does not necessarily reflect the views of the agency, and no official endorsement should be inferred. Mention of trade names or commercial products does not constitute an endorsement or recommendation for use.

Supporting Information Available

Dilution ratio calculation scheme, concentrations calculation and uncertainty, engine load calculation, tables of data, figures, and references. This material is available free of charge via the Internet at http://pubs.acs.org.

Literature Cited

(1) Dockery, D. W.; Pope, C. A.; Xu, X. P.; Spengler, J. D.; Feiirs, B. G. An association between air-pollution and mortality in 6 United-States cities. *New Engl. J. Med.* **1993**, *329*, 1753−1759.

(2) Vedal, S. Ambient particles and health: Lines that divide. *J. Air Waste Manage.* **1997**, *47*, 551−581.

(3) Kleinman, M. T.; Hamade, A.; Meacher, D.; Oldham, M.; Sioutas, C.; Chakrabarti, L.; Stram, D.; Froines, J. R.; Cho, A. K. Inhalation of concentrated ambient particulate matter near a heavily trafficked road stimulates antigen-induced airway responses in mice. *J. Air Waste Manage.* **2005**, *55*, 1277−1288.

(4) Li, N.; Sioutas, C.; Cho, A.; Schmitz, D.; Misra, C.; Sempf, J.; Wang, M. Y.; Oberley, T.; Froines, J.; Nel, A. Ultrafine particulate pollutants induce oxidative stress and mitochondrial damage. *Environ. Health Persp.* **2003**, *111*, 455−460.

(5) Donaldson, K.; Stone, V.; Clouter, A.; Renwick, L. Ultrafine particles. *Occup. Environ. Med.* **2001**, *58*, 211.

(6) Oberdorster, G. Pulmonary effects of inhaled ultrafine particles. *Int. Arch. Occup. Environ. Health* **2001**, *74*, 1−8.

(7) Ntziachristos, L.; Mamakos, A.; Samaras, Z.; Rexeis, M. Diesel particle exhaust emissions from light duty vehicles and heavy duty engine. *J. Fuels Lubricants* **2006**, SAE Technical Paper 2006-01-0866.

(8) Maricq, M. M.; Podsiadlik, D. H.; Chase, R. E. Gasoline Vehicle Particle Size Distributions: Comparison of Steady State, FTP, and US06 Measurements. *Environ. Sci. Technol.* **1999**, *33*, 2007−2015.

(9) Zhu, Y. F.; Hinds, W. C.; Shen, S.; Sioutas, C. Seasonal trends of concentration and size distribution of ultrafine particles near major highways in Los Angeles. *Aerosol Sci. Technol.* **2004**, *38*, 5−13.

(10) Westerdahl, D.; Fruin, S.; Sax, T.; Fine, P. M.; Sioutas, C. Mobile platform measurements of ultrafine particles and associated pollutant concentrations on freeways and residential streets in Los Angeles. *Atmos. Environ.* **2005**, *39*, 3597−3610.

(11) Hitchins, J.; Morawska, L.; Wolff, R.; Gilbert, D. Concentrations of submicrometre particles from vehicle emissions near a major road. *Atmos. Environ.* **2000**, *34*, 51−59.

(12) Schauer, J. J.; Rogge, W. F.; Hildemann, L. M.; Mazurek, M. A. Source apportionment of airborne particulate matter using organic compounds as tracers. *Atmos. Environ.* **1996**, *30*, 3837−3855.

(13) Cyrys, J.; Stolzel, M.; Heinrich, J.; Kreyling, W. G.; Menzel, N.; Wittmaack, K.; Tuch, T.; Wichmann, H. E. Elemental composition and sources of fine and ultrafine ambient particles in Erfurt, Germany. *Sci. Total Environ.* **2003**, *305*, 143−156.

(14) Shi, J. P.; Harrison, R. M. Investigation of ultrafine particle formation during diesel exhaust dilution. *Environ. Sci. Technol.* **1999**, *33*, 3730−3736.

(15) Arhami, M.; Kuhn, T.; Fine, P. M.; Delfino, R. J.; Sioutas, C. Effects of sampling artifacts and operating parameters on the performance of a semicontinuous particulate elemental carbon/organic carbon monitor. *Environ. Sci. Technol.* **2006**, *40*, 945−954.

(16) Zhu, Y. F.; Hinds, W. C.; Kim, S.; Shen, S.; Sioutas, C. Study of ultrafine particles near a major highway with heavy-duty diesel traffic. *Atmos. Environ.* **2002**, *36*, 4323−4335.

(17) Hering, S. V.; Miguel, A. H.; Dod, R. L. Tunnel Measurements of the PAH, Carbon Thermogram and Elemental Source Signature for Vehicular Exhaust. *Sci. Total Environ.* **1984**, *36*, 39−45.

(18) Weingartner, E.; Keller, C.; Stahel, W. A.; Burtscher, H.; Baltensperger, U. Aerosol emission in a road tunnel. *Atmos. Environ.* **1997**, *31*, 451−462.

(19) Funasaka, K.; Miyazaki, T.; Kawaraya, T.; Tsuruho, K.; Mizuno, T. Characteristics of particulates and gaseous pollutants in a highway tunnel. *Environ. Pollut.* **1998**, *102*, 171−176.

(20) Geller, M. D.; Biswas, S.; Sioutas, C. Determination of particle effective density in urban environments with a differential mobility analyzer and aerosol particle mass analyzer. *Aerosol Sci. Technol.* **2006**, *40*, 709−723.

(21) Ntziachristos, L. Z. Samaras. *Copert III - Computer programme to calculate emissions from road transport.* Technical Report 49; European Environment Agency: Copenhagen, Denmark, 2000; p 86.

(22) Harrison, R. M.; Jones, M.; Collins, G. Measurements of the physical properties of particles in the urban atmosphere. *Atmos. Environ.* **1999**, *33*, 309−321.

(23) Kuhn, T.; Biswas, S.; Sioutas, C. Diurnal and seasonal characteristics of particle volatility and chemical composition in the vicinity of a light-duty vehicle freeway. *Atmos. Environ.* **2005**, *39*, 7154−7166.

(24) Geller, M. D.; Sardar, S. B.; Phuleria, H.; Fine, P. M.; Sioutas, C. Measurements of particle number and mass concentrations and size distributions in a tunnel environment. *Environ. Sci. Technol.* **2005**, *39*, 8653−8663.

(25) Kurniawan, A.; Schmidt-Ott, A. Monitoring the soot emissions of passing cars. *Environ. Sci. Technol.* **2006**, *40*, 1911−1915.
(26) Kirchstetter, T. W.; Harley, R. A.; Kreisberg; N. M.; Stolzenburg, M. R.; et al. On-road measurement of fine particle and nitrogen oxide emissions from light- and heavy-duty motor vehicles. *Atmos. Environ.* **1999**, *33*, 2955−2968.
(27) Zhang, K. M.; Wexler, A. S. Evolution of particle number distribution near roadways−Part I: analysis of aerosol dynamics and its implications for engine emission measurement. *Atmos. Environ.* **2004**, *38*, 6643−6653.
(28) Kuhns, H. D.; Mazzoleni, C.; Moosmuller, H.; Nikolic, D.; Keislar, R. E.; Barber, P. W.; Li, Z.; Etyemezian, V.; Watson, J. G. Remote sensing of PM, NO, CO and HC emission factors for on-road gasoline and diesel engine vehicles in Las Vegas, NV. *Sci. Total Environ.* **2004**, *322*, 123−137.
(29) Kittelson, D. B.; Watts, W. F.; Johnson, J. P. Nanoparticle emissions on Minnesota highways. *Atmos. Environ.* **2004**, *38*, 9−19.
(30) Zielinska, B.; Sagebiel, J.; Arnott; W. P.; Rogers, C. F.; Kelly, K. E.; Wagner, D. A.; Lighty, J. S.; Sarofim, A. F.; Palmer, G. Phase and size distribution of polycyclic aromatic hydrcarbons in diesel and gasoline vehicle emissions. *Environ. Sci. Technol.* **2004**, *38*, 2557−2567.
(31) Vogt, R.; Scheer, V.; Casati, R.; Bender, T. On-road measurement of particle emission in the exhaust plume of a diesel passenger car. *Environ. Sci. Technol.* **2003**, *37*, 4070−4076.
(32) Rönkkö, T.; Virtanen, A.; Vaaraslahti, K.; Keskinen, J.; Pirjola, L.; Lappi, M. Effect of dilution conditions and driving parameters on nucleation mode particles in diesel exhaust: Laboratory and on-road study. *Atmos. Environ.* **2006**, *40*, 2893−2901.
(33) Giechaskiel, B.; Ntziachristos, L.; Samaras, Z.; Scheer, V.; Casati, R.; Vogt, R. Formation potential of vehicle exhaust nucleation mode particles on-road and in the laboratory. *Atmos. Environ.* **2005**, *39*, 3191−3198.
(34) Mozurkewich, M.; Chan, T. W.; Aklilu, Y. A.; Verheggen, B. Aerosol particle size distributions in the lower Fraser Valley: evidence for particle nucleation and growth. *Atmos. Chem. Phys.* **2004**, *4*, 1047−1062.
(35) Thompson, N.; Ntziachristos, L.; Samaras, Z.; Aakko, P. Overview of the European "Particulates" project on the characterization of exhaust particulate emissions from road vehicles: results for heavy-duty engines. *SAE Technology Paper* **2004**, 2004-01-1986.
(36) Phuleria, H. C.; Geller, M. D.; Fine, P. M.; Sioutas, C. Size-resolved emissions of organic tracers from light- and heavy-duty vehicles measured in a California roadway tunnel. *Environ. Sci. Technol.* **2006**, *40*, 4109−4118.

Received for review October 27, 2006. Revised manuscript received December 19, 2006. Accepted January 19, 2007.

ES062590S